

# Interactions Between Mn<sub>12</sub>-ac and Thin Gold Films: Using Mn<sub>12</sub>-ac as Scattering Centers

Joel Means\* and Winfried Teizer†

*Department of Physics, Texas A&M University, College Station, TX 77843-4242*

We explore the electronic interactions between a thin gold film and a surface layer of the molecular magnet Mn<sub>12</sub>-acetate. Magnetoresistance measurements of the gold allow characterization of the interactions by comparison with the theoretical predictions of weak localization. We find that the presence of Mn<sub>12</sub>-acetate on the surface of the gold film leads to a reduction in elastic scattering while increasing the spin scattering of the conduction electrons. This is the first experimental evidence of molecular magnets being used as scattering centers for an adjacent metallic film.

PACS numbers: 73.20.Fz, 73.43.Qt, 73.61.At, 75.50.Xx

## INTRODUCTION

Manganese-12 acetate (Mn<sub>12</sub>-ac) is a molecular magnet which has been the subject of much study, both theoretically [1, 2, 3, 4, 5, 6, 7, 8, 9, 10, 11] and experimentally [12, 13, 14, 15, 16, 17, 18], since it was first fabricated by Lis in 1980 [19]. While most of the research into the properties of Mn<sub>12</sub>-ac has been focused on its interesting magnetic properties, some work has been done more recently exploring the electronic properties, in particular the conductance through Mn<sub>12</sub>-ac [20, 21, 22, 23, 24]. Theoretical predictions have also been made concerning the electronic structure of related Mn<sub>12</sub> molecules [4, 25]. This study seeks to shed light on how the presence of these molecular magnets on the surface of a gold film can affect the transport properties of the conduction electrons within that gold film.

In order to explore the interactions between the Mn<sub>12</sub>-ac and the gold film, one must have a theoretical framework for understanding the interactions. The theory of weak localization [26, 27, 28, 29] provides such a framework by quantifying the strengths of the various scattering processes experienced by the conduction electrons. Conduction electrons within a metal can undergo elastic scattering, such as surface scattering or scattering from lattice defects; inelastic scattering, such as electron-phonon scattering; spin scattering, such as scattering from magnetic impurities; or spin-orbit scattering. Each of these processes makes specific contributions to the resistance of the film and each changes in a specific way in the presence of a magnetic field. Weak localization predicts the change in resistance of a metallic film in a perpendicular magnetic field,  $H_{\perp}$ , due to weak localization effects to have the following dependence [30]:

$$\frac{\Delta R(H_{\perp})}{R} = \frac{e^2 R_{\square}}{2\pi^2 \hbar} \times \left[ \psi\left(\frac{1}{2} + \frac{H_1}{H_{\perp}}\right) - \psi\left(\frac{1}{2} + \frac{H_2}{H_{\perp}}\right) + \frac{1}{2}\psi\left(\frac{1}{2} + \frac{H_3}{H_{\perp}}\right) - \frac{1}{2}\psi\left(\frac{1}{2} + \frac{H_2}{H_{\perp}}\right) \right] \quad (1)$$

where  $R_{\square}$  is the sheet resistance of the film and  $H_n$  are characteristic fields given by

$$H_1 = H_0 + H_{so} + H_s \quad (2)$$

$$H_2 = \frac{4}{3}H_{so} + \frac{2}{3}H_s + H_i \quad (3)$$

$$H_3 = 2H_s + H_i \quad (4)$$

with  $H_0$ ,  $H_{so}$ ,  $H_s$ , and  $H_i$  being characteristic fields corresponding to elastic, spin-orbit, spin, and inelastic scattering, respectively. The physical quantity of interest is

the scattering time,  $\tau_n$ , associated with each type of scattering process. The scattering times are related to the scattering fields by

$$H_n \tau_n = \frac{\hbar}{4eD} \quad (5)$$

where  $e$  is the electron charge and  $D$  is the diffusion constant in two dimensions. Measurement of the magnetoresistance of a metal, then, allows one to determine the scattering times associated with the various scattering processes which the conduction electrons undergo. By simultaneously measuring the magnetoresistance of gold films with and without Mn<sub>12</sub>-ac on the surface and computing how the characteristic scattering times change, one can determine the types of interactions taking place

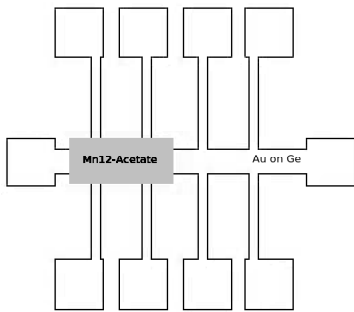


Figure 1: Schematic of pattern used for Au samples.

between the conduction electrons in the gold and the  $\text{Mn}_{12}\text{-ac}$ .

## EXPERIMENTAL SETUP AND RESULTS

In order to perform the magnetoresistance measurements, a thin film of Au was made by thermal evaporation onto a room temperature silicon substrate with the native oxide layer and a 20Å Ge adhesion layer. A shadow mask, as illustrated in figure 1, was used to define a pattern consisting of a single current-carrying strip with eight voltage probes, four on each side of the strip. This setup allows a four-wire measurement of two different sections of the strip simultaneously and with some redundancy. By placing  $\text{Mn}_{12}\text{-ac}$  on half of the current carrying strip, the magnetoresistance with and without  $\text{Mn}_{12}\text{-ac}$  can be measured simultaneously using the same excitation current and magnetic field. Theoretical fits are obtained using a least-squares fitting method to obtain the best set of the four fitting parameters,  $H_0$ ,  $H_{so}$ ,  $H_i$ , and  $H_s$ .

$\text{Mn}_{12}\text{-ac}$  was placed on the surface of the Au film using a simple drop-and-dry technique, similar to the established dip-and-dry technique[31, 32]. A solution was made by dissolving 10 mg of  $\text{Mn}_{12}\text{-ac}$  powder in 10 ml of isopropyl alcohol. Five drops of this solution were dropped onto half of the Au film with ample drying time between drops. It was observed by AFM (see Figure 1, ref. 32) that this is sufficient to ensure good coverage of the Au with  $\text{Mn}_{12}\text{-ac}$ . Samples were then mounted in a dilution refrigerator for measurement. Results shown are from typical samples.

Figure 2 shows the measured magnetoresistance for a 7.8 nm Au film, with and without  $\text{Mn}_{12}\text{-ac}$ , at a temperature of 600 mK. In the dilution refrigerator used in these experiments, 600 mK was found to be an easy temperature to reach and stabilize, while lower temperature measurements did not seem to provide any substantial advantage. The solid curves are fits to the theory of weak localization using Equation 1. The fitting parameters,  $H_n$ , used for the fits in Figure 2 are listed in Table I. Also listed are the characteristic scattering times

calculated using Equation 5. The elastic scattering time is increased by approximately a factor of two if  $\text{Mn}_{12}$  is present. This indicates a decrease in the amount of elastic scattering, consistent with a change in the surface scattering, while the spin-orbit scattering are essentially unchanged, while the spin scattering time is reduced by around an order of magnitude. This indicates a significant increase in the amount of spin scattering taking place. The decrease in elastic scattering and increase in spin scattering are consistent with a picture in which electrons which would have scattered from the surface of the Au film are instead entering the  $\text{Mn}_{12}\text{-ac}$  molecules and undergoing spin scattering, most likely from the Mn atoms within the molecules.

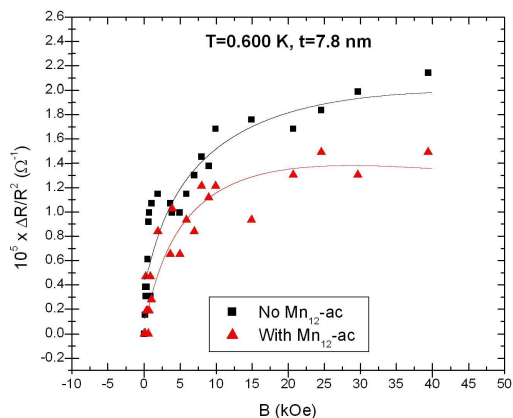


Figure 2: Magnetoresistance of 7.8 nm Au film at 600 mK. Solid curves are fits to theory.

	No $\text{Mn}_{12}\text{-ac}$	With $\text{Mn}_{12}\text{-ac}$
$H_0$	$12.9 \pm 0.5$	$4.3 \pm 0.2$
$H_i$	$0.0145 \pm 0.005$	$0.0090 \pm 0.0045$
$H_{so}$	$0.97 \pm 0.02$	$0.58 \pm 0.02$
$H_s$	$0.0040 \pm 0.0025$	$0.0080 \pm 0.0020$
$\tau_0$	$(3.62 \pm 0.07) \times 10^{-15}$	$(6.31 \pm 0.15) \times 10^{-15}$
$\tau_i$	$(3.66 \pm 1.20) \times 10^{-12}$	$(3.97 \pm 1.92) \times 10^{-12}$
$\tau_{so}$	$(4.85 \pm 0.01) \times 10^{-14}$	$(4.76 \pm 0.05) \times 10^{-14}$
$\tau_s$	$(1.91 \pm 1.17) \times 10^{-11}$	$(3.59 \pm 0.82) \times 10^{-12}$

Table I: Characteristic fields and scattering times for 7.8 nm gold film at 600 mK.

Figure 3 shows the magnetoresistance for a 9.0 nm Au film, also at 600 mK. Fitting parameters used for the solid curves are listed in Table II. As with the thinner sample, the inelastic and spin-orbit scattering times remain unchanged within experimental error. It should

be noted that due to the small changes being measured, we observe digitization of the data, indicating that the measurements are close to the experimental resolution. The changes in resistance were on the order of the smallest digit which could be resolved with the experimental setup used. This digitization also leads to larger relative errors in the numbers reported. Again, there is a significant increase in the elastic scattering times, by a factor of approximately four. There is also a decrease in the spin scattering time by about an order of magnitude. This behavior is consistent with that seen for the thinner sample.

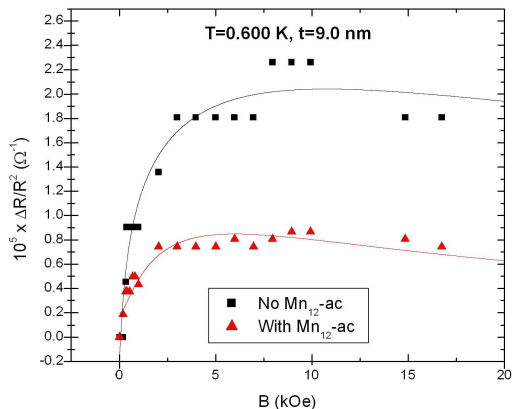


Figure 3: Magnetoresistance of 9.0 nm Au film at 600 mK. Solid curves are fits to theory.

	No $Mn_{12-ac}$	With $Mn_{12-ac}$
$H_0$	$3.1 \pm 0.4$	$0.5 \pm 0.1$
$H_i$	$0.0015 \pm 0.001$	$0.0050 \pm 0.0045$
$H_{so}$	$0.23 \pm 0.02$	$0.12 \pm 0.02$
$H_s$	$0.0005 \pm 0.0004$	$0.0050 \pm 0.0030$
$\tau_0$	$(7.47 \pm 0.48) \times 10^{-15}$	$(1.88 \pm 0.18) \times 10^{-15}$
$\tau_i$	$(2.63 \pm 1.66) \times 10^{-11}$	$(8.78 \pm 7.72) \times 10^{-12}$
$\tau_{so}$	$(9.99 \pm 0.21) \times 10^{-14}$	$(7.75 \pm 0.51) \times 10^{-14}$
$\tau_s$	$(4.60 \pm 2.16) \times 10^{-11}$	$(2.70 \pm 1.43) \times 10^{-12}$

Table II: Characteristic fields and scattering times for 9.0 nm gold film at 600 mK.

As a control experiment, a gold sample was prepared with pure isopropyl alcohol on half of the current carrying path in order to eliminate the possibility of the effect being due to residual contaminations in the isopropyl alcohol. The experimental data, along with theoretical fits, are shown in Figure 4. The fitting parameters which provided the best fit are listed in table III. Within experimental error, there are no significant changes in any of

the scattering times due to the presence of the isopropyl alcohol or to any contaminations within the isopropyl alcohol. This indicates that the changes seen in the samples with  $Mn_{12-ac}$  are due to the  $Mn_{12-ac}$  and not to the isopropyl alcohol which was used as a solvent for sample preparation.

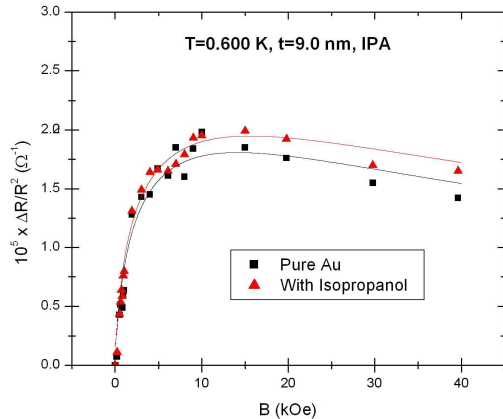


Figure 4: Magnetoresistance of 9.0 nm Au film at 600 mK with isopropyl alcohol. Solid curves are fits to theory.

	Pure Au	With Isopropyl Alcohol
$H_0$	$3.2 \pm 0.2$	$3.6 \pm 0.4$
$H_i$	$0.0035 \pm 0.0015$	$0.0015 \pm 0.0010$
$H_{so}$	$0.29 \pm 0.02$	$0.30 \pm 0.02$
$H_s$	$0.0010 \pm 0.0005$	$0.0010 \pm 0.0005$
$\tau_0$	$(7.30 \pm 0.25) \times 10^{-15}$	$(6.92 \pm 0.38) \times 10^{-15}$
$\tau_i$	$(6.67 \pm 1.85) \times 10^{-12}$	$(2.86 \pm 1.81) \times 10^{-11}$
$\tau_{so}$	$(8.05 \pm 0.34) \times 10^{-14}$	$(8.25 \pm 0.09) \times 10^{-14}$
$\tau_s$	$(2.33 \pm 1.40) \times 10^{-11}$	$(3.21 \pm 1.46) \times 10^{-11}$

Table III: Characteristic fields and scattering times for 9.0 nm gold film at 600 mK with isopropyl alcohol.

## CONCLUSION

It has been shown that the presence on  $Mn_{12-ac}$  on the surface of a thin Au film causes significant changes in the magnetoresistance of the Au film. Fitting of the experimental data to the predictions of the theory of weak localization allows characterization of the types of changes taking place. In particular, there is an enhancement of the spin scattering of the conduction electrons, coupled with a reduction in the elastic scattering. This is consistent with electrons entering the  $Mn_{12-ac}$  and undergoing spin scattering, rather than simply scattering from the

surface of the Au film. This is the first time that experimental evidence has been seen indicating that a surface layer of molecular magnets can be used as scattering centers to change the electron transport properties of a metallic film.

---

\* Currently at Sandia National Labs, Albuquerque, NM 87185-1084

† Electronic address: teizer@tamu.edu

- [1] J. Villain, F. Hartman-Boutron, R. Sessoli, and A. Rettori, *Europhys. Lett.* **27**, 159 (1994).
- [2] P. Politi, A. Rettori, F. Hartmann-Boutron, and J. Villain, *Phys. Rev. Lett.* **75**, 537 (1995).
- [3] D. A. Garanin and E. M. Chudnovsky, *Phys. Rev. B* **56**, 11102 (1997).
- [4] Z. Zeng, D. Guenzburger, and D. E. Ellis, *Phys. Rev. B* **59**, 6927 (1999).
- [5] T. Goto, T. Kubo, T. Koshiba, Y. Fujii, A. Oyamada, J. Arai, K. Takeda, and K. Awaga, *Physica B: Cond. Mat.* **284-288**, Part 2, 1227 (2000).
- [6] T. Pohjola and H. Schoeller, *Physica B: Cond. Mat.* **284-288**, Part 2, 1223 (2000).
- [7] J. Tejada, *Polyhedron* **20**, 1751 (2001).
- [8] J. Liu, B. Wu, L. Fu, R. B. Diener, and Q. Niu, *Phys. Rev. B* **65**, 224401 (2002).
- [9] M. R. Pederson, N. Bernstein, and J. Kortus, *Phys. Rev. Lett.* **89**, 097202 (2002).
- [10] A. V. Postnikov, J. Kortus, and M. R. Pederson, *Phys. Status Solidi B* **243**, 2533 (2006).
- [11] J. Kortus, *C. R. Chim.* **10**, 65 (2007).
- [12] A. Caneschi, D. Gatteschi, R. Sessoli, A. L. Barra, L. C. Brunel, and M. Guillot, *J. Am. Chem. Soc.* **113**, 5873 (1991).
- [13] R. Sessoli, D. Gatteschi, A. Caneschi, and M. A. Novak, *Nature* **365**, 141 (1993).
- [14] B. Barbara, W. Wernsdorfer, L. Sampaio, J.-G. Park, C. Paulsen, M. A. Novak, R. Ferré, D. Mailly, R. Sessoli, A. Caneschi, et al., *J. Magn. Magn. Mater.* **140-144**, 1825 (1995).
- [15] C. Paulsen and J.-G. Park, in *Quantum Tunneling of Magnetization - QTM '94*, edited by L. Gunther and B. Barbara (Kluwer Academic Publishers, Dordrecht, the Netherlands, 1995), pp. 189-207.
- [16] C. Paulsen, J.-G. Park, B. Barbara, R. Sessoli, and A. Caneschi, *J. Magn. Magn. Mater.* **140-144**, 379 (1995).
- [17] M. A. Novak and R. Sessoli, in *Quantum Tunneling of Magnetization - QTM '94*, edited by L. Gunther and B. Barbara (Kluwer Academic Publishers, Dordrecht, the Netherlands, 1995), pp. 171-188.
- [18] M. A. Novak, R. Sessoli, A. Caneschi, and D. Gatteschi, *J. Magn. Magn. Mater.* **146**, 211 (1995).
- [19] T. Lis, *Acta Cryst.* **B 36**, 2042 (1980).
- [20] M.-H. Jo, J. Grose, K. Baheti, M. Deshmukh, J. Sokol, E. Rumberger, D. Hendrickson, J. Long, H. Park, and D. Ralph, *Nano Lett.* **6**, 2014 (2006).
- [21] M. N. Leuenberger and E. R. Mucciolo, *Phys. Rev. Lett.* **97**, 126601 (2006).
- [22] H. B. Heersche, Z. de Groot, J. A. Folk, H. S. J. van der Zant, C. Romeike, M. R. Wegewijs, I. Zobbi, D. Barreca, E. Tondello, and A. Cornia, *Phys. Rev. Lett.* **96**, 206801 (2006).
- [23] C. Ni, S. Shah, D. Hendrickson, and P. R. Bandaru, *Appl. Phys. Lett.* **89**, 212104 (2006).
- [24] C. Romeike, M. R. Wegewijs, W. Hofstetter, and H. Schoeller, *Phys. Rev. Lett.* **97**, 206601 (2006).
- [25] S. Voss, M. Fonin, U. Rudiger, M. Burgert, and U. Groth, *Appl. Phys. Lett.* **90**, 133104 (2007).
- [26] E. Abrahams, P. W. Anderson, D. C. Licciardello, and T. V. Ramakrishnan, *Phys. Rev. Lett.* **42**, 673 (1979).
- [27] S. Hikami, A. I. Larkin, and Y. Nagaoka, *Prog. Theor. Phys.* **63**, 707 (1980).
- [28] P. A. Lee and T. V. Ramakrishnan, *Phys. Rev. B* **26**, 4009 (1982).
- [29] G. Bergmann, *Phys. Rev. B* **28**, 2914 (1983).
- [30] N. Giordano and M. A. Pennington, *Phys. Rev. B* **47**, 9693 (1993).
- [31] K. Kim, D. M. Seo, J. Means, V. Meenakshi, W. Teizer, H. Zhao, and K. R. Dunbar, *Appl. Phys. Lett.* **85**, 3872 (2004).
- [32] D. Seo, V. Meenakshi, W. Teizer, H. Zhao, and K. Dunbar, *J. Magn. Magn. Mater.* **301**, 31 (2006).